



Published in final edited form as:

Transl Res. 2016 April ; 170: 99–111. doi:10.1016/j.trsl.2015.12.009.

## M10, a Caspase Cleavage Product of the Hepatocyte Growth Factor Receptor, Interacts with Smad2 and Demonstrates Anti-Fibrotic Properties *in Vitro* and *in Vivo*

Ilia Atanelishvili<sup>1,\*</sup>, Yuichiro Shirai<sup>1,2,\*</sup>, Tanjina Akter<sup>1</sup>, Taylor Buckner<sup>1,3,4</sup>, Atsushi Noguchi<sup>1</sup>, Richard M. Silver<sup>1</sup>, and Galina S. Bogatkevich<sup>1</sup>

<sup>1</sup>Division of Rheumatology and Immunology, Department of Medicine, Medical University of South Carolina, Charleston, South Carolina, USA

<sup>2</sup>Nippon Medical School Department of Allergy and Rheumatology, Tokyo, Japan

<sup>3</sup>South Carolina Governor's School for Science & Mathematics

<sup>4</sup>Honors College at the College of Charleston, USA

### Abstract

Hepatocyte growth factor receptor, also known as cellular mesenchymal-epithelial transition factor (c-MET, MET), is an important antifibrotic molecule that protects various tissues, including lung, from injury and fibrosis. The intracellular cytoplasmic tail of MET contains a caspase-3 recognition motif “DEVD-T” that upon cleavage by caspase-3 generates a 10 amino acid peptide, TRPASFWETS, designated as “M10”. M10 contains at its N-terminus the uncharged amino acid proline (P) directly after a cationic amino acid arginine (R) which favors the transport of the peptide through membranes. M10, when added to cell culture medium, remains in the cytoplasm and nuclei of cells for up to 24 hours. M10 effectively decreases collagen in both scleroderma and TGFβ-stimulated normal lung and skin fibroblasts. M10 interacts with the MH2 domain of Smad2 and inhibits TGFβ-induced Smad2 phosphorylation, suggesting that the antifibrotic effects of M10 are mediated in part by counteracting Smad-dependent fibrogenic pathways. In the bleomycin murine model of pulmonary fibrosis, M10 noticeably reduced lung inflammation and fibrosis. Ashcroft fibrosis scores and lung collagen content were significantly lower in bleomycin-treated mice receiving M10 as compared with bleomycin-treated mice receiving scrambled peptide. We conclude that M10 peptide interacts with Smad2 and demonstrates strong antifibrotic effects *in vitro* and *in vivo* in an animal model of lung fibrosis and should be considered as a potential therapeutic agent for systemic sclerosis and other fibrosing diseases.

---

Address correspondence and reprint request to: Galina S. Bogatkevich, MD, PhD, 96 Jonathan Lucas Street, Suite 816, Medical University of South Carolina, Charleston, SC 29425, Tel.: (843) 792-7631, Fax: (843) 792-7121, bogatkev@musc.edu.

\*I. Atanelishvili and Y. Shirai contributed equally to this work

**Publisher's Disclaimer:** This is a PDF file of an unedited manuscript that has been accepted for publication. As a service to our customers we are providing this early version of the manuscript. The manuscript will undergo copyediting, typesetting, and review of the resulting proof before it is published in its final citable form. Please note that during the production process errors may be discovered which could affect the content, and all legal disclaimers that apply to the journal pertain.

## Introduction

Scleroderma (systemic sclerosis, SSc) is an autoimmune disease characterized by fibrotic changes of skin and internal organs. The molecular mechanisms underlying the pathogenesis of SSc are not well understood, and treatment is often toxic and inefficacious.<sup>1,2</sup> Earlier studies have identified hepatocyte growth factor (HGF) as an antifibrotic agent that protects against tissue fibrosis in several animal models.<sup>3-5</sup> We previously demonstrated that antifibrotic effects mediated by the HGF receptor, also known as cellular mesenchymal-epithelial transition factor (c-MET, MET), are impaired in lung fibroblasts isolated from a subset of scleroderma patients with severe interstitial lung disease (ILD).<sup>6</sup> We recently observed that lung fibroblasts from some SSc-ILD patients with poor pulmonary outcomes express the D1398G variant of the MET receptor, and that a D1398G MET receptor mutant generated in vitro does not exert antifibrotic effects of MET in lung fibroblasts.<sup>7</sup>

MET is a transmembrane protein and a member of the receptor tyrosine kinase class IV, transducing signals from extracellular matrix into the cytoplasm. The fully processed MET protein is composed of a 50 kD  $\alpha$ -chain and a 145 kD  $\beta$ -chain linked by a disulfide bridge. The  $\alpha$ -chain and the N-terminal part of the  $\beta$ -chain form the extracellular domain. The remainder of the  $\beta$ -chain forms transmembrane and tyrosine kinase domains and a C-terminal tail.<sup>8,9</sup>

MET is a high affinity receptor for HGF, a polypeptide growth factor from the plasminogen family. The binding of HGF to MET induces kinase catalytic activity that triggers autophosphorylation at the kinase domain and initiates receptor activation. Phosphorylated kinase domain works as a docking site for downstream signaling molecule and activates several signaling cascades including Ras-Erk, PI3 kinase-Akt, or PLC gamma-PKC.<sup>9</sup> HGF/MET signaling plays significant roles in embryo development, tissue repair, cell proliferation, migration, differentiation, mitogenesis, morphology and survival.<sup>9,10</sup> MET-mediated pleiotropic signaling depends in part on the ability of MET to form heterodimers with other cell surface receptors such as CD44,  $\beta$ 4-integrin, Fas-receptor, and semaphorin-receptor.<sup>11-15</sup>

Increased expression of MET in scleroderma fibroblasts and other myofibroblasts has been well documented.<sup>16,17</sup> Foveau et al. demonstrated that MET, when overexpressed, could activate endogenous cysteine-dependent aspartate-directed proteases (caspases) following stress conditions in several cell lines;<sup>18</sup> other research groups showed that the MET receptor mediates HGF-induced apoptosis in lung and liver myofibroblasts.<sup>19,20</sup>

Caspase-3 plays a key effector role in apoptosis by cleaving specific substrates important for downstream apoptosis signaling<sup>21</sup> and has some additional functions including B cell regulation and T cell differentiation.<sup>22,23</sup> An autoantibody against caspase-3 is generated in SSc, and this antibody has been correlated to the severity of SSc-ILD, vascular damage, and inflammation.<sup>25</sup> Activated caspase-3 recognizes aspartic acid-containing motifs within MET and cleaves those generating several stable fragments of the MET receptor that have been implicated in regulation of cell apoptosis and MET expression.<sup>18,25,26</sup> Upon cleavage by caspase-3, the intracellular cytoplasmic tail of MET generates a 10 amino acid peptide,

TRPASFWETS, designated as “M10”. The present study was undertaken to investigate the signaling pathways underlying antifibrotic effects of M10 in lung and skin fibroblasts.

## Materials and Methods

### Materials

M10 and 10 amino acids scrambled peptides were obtained from GenScript (Piscataway, NJ), red fluorescent 5,6- carboxytetramethyl-rhodamine, succinimidyl ester (5,6-TAMRA)-conjugated M10 was purchased from BioSynthesis (Lewisville, Texas). Anti-type I collagen antibody was from Southern Biotechnology (Birmingham, AL), anti-Met (C12) antibody was from Santa Cruz Biotechnology (Santa Cruz, CA), anti-Smad2 and anti-phospho-Smad2 was from Cell Signaling Technology (Danvers, MA), anti- $\beta$ -actin was from Sigma (St. Louis, MO). Alexa Fluor 647® conjugated goat anti-rabbit secondary antibody, Alexa Fluor 488® Phalloidin, and ProLong® Gold anti-fade mountant with DAPI were obtained from Life Technologies (Grand Island, NY). Recombinant human Smad2 (NM\_005901) with C-terminal MYC/DDK tag, Smad4 (NM\_005359) with C-terminal MYC/DDK tag, and anti-DDK antibody were purchased from OriGene Technologies (Rockville, MD), TGF $\beta$  was from R&D Systems (Minneapolis, MN), bleomycin sulfate was from Hospira Inc. (Lake Forest, IL). ApoSENSOR™ Cell Viability Assay Kit was obtained from BioVision (Milpitas, CA).

### Cell Culture

Lung tissues were collected postmortem from three SSc patients who fulfilled the 2013 ACR/EULAR classification criteria for SSc<sup>27</sup> and had evidence of lung involvement according to guidelines of the Institutional Review Board of the Medical University of South Carolina (MUSC). The diagnosis of SSc-ILD was confirmed by histological examination of postmortem lung tissue. Lung fibroblasts were isolated from scleroderma lung tissue and from normal controls as previously described<sup>28</sup> and used between second and fourth passages in all experiments. Human fetal lung fibroblasts MRC5 were purchased from Sigma (St. Louis, MO), human lung adenocarcinoma epithelial cells A549 were purchased from Lonza (Walkersville, MD).

Skin fibroblasts were isolated from 3-mm skin biopsies obtained from the involved forearm skin of three scleroderma patients and from age-, sex-, and race-matched healthy adult donors according to guidelines of the MUSC IRB. Skin was cleared of fat and hair, diced (0.5 × 0.5 mm pieces), and cultured in Dulbecco’s modified Eagle’s medium (DMEM; Gibco, Grand Island, NY) supplemented with 20% fetal bovine serum (FBS), 2 mM l-glutamine, gentamicin sulfate (50 $\mu$ g/ml), and amphotericin B (5 $\mu$ g/ml) at 37°C in 5%CO<sub>2</sub>. Medium was changed every five days to remove dead and non-attached cells until fibroblasts reached confluence. Monolayer cultures were maintained in the 10% FBS DMEM.

### Cell Viability Assay and Trypan Blue Cell Counting

Normal and scleroderma lung and skin fibroblasts, MRC5, and A549 cells were cultured in 12-well plates, serum-starved, and incubated overnight with different concentrations of M10

or scrambled peptide. Cisplatin (50  $\mu\text{M}$ ) was used as a drug, known to reduce cell viability. Cells were collected with trypsin, re-suspended in cell culture medium (0.5ml/well), and aliquoted for ApoSENSOR™ cell viability assay and trypan blue cell counting assay. For cell viability assay, 10  $\mu\text{l}$  of cell suspension was transferred to the white-walled 96-well luminometer plate and mixed with 100  $\mu\text{l}$  of Nucleotide releasing buffer followed by adding 10ul of ATP monitoring enzyme. The ATP/luciferin-generated signals were measured by a luminometer. Data were expressed as a relative light unit normalized by the signal received from the cells incubated in serum-free medium for each individual cell line. For cell counts, 100  $\mu\text{l}$  of cell suspension was mixed with Trypan blue solution at a ratio of 1:1. Viable cells were counted under light microscopy using hemocytometer. The number of cells per well was calculated on the basis of a dilution factor that was identical for all groups.

### Immunofluorescent studies

Cells were cultured to subconfluence on glass slides, serum-starved overnight, and incubated with M10 or 5,6-TAMRA-M10 with and without TGF $\beta$  for 24 hours. Cells were fixed with 4% formaldehyde and blocked with PBS containing 5%BSA, 0.1% Triton, and 0.0004% Sodium Azide. A part of the slides were immunostained with anti-MET C12 antibody or with anti-Smad2 antibody followed by Alexa Fluor 647® conjugated goat anti-rabbit secondary antibody. Next, slides were washed with PBS and incubated with Alexa Fluor 488® phalloidin for 30 minutes (dilution in PBS 1:50). The labeled slide was mounted with ProLong Gold anti-fade reagent with DAPI and visualized under Olympus FV10i laser scanning confocal or Zeiss Axio Imager M2 microscope system.

### Preparation of cell extracts, immunoprecipitation, and immunoblotting

Cells were collected and analyzed by immunoblotting as previously described.<sup>28,29</sup> The phosphorylation of Smad2 was analyzed by Western blot using anti-phospho-Smad2 antibody in accordance with the manufacturer's instructions (Cell Signaling Technology). Briefly, lung and skin fibroblasts were cultured on 6-well plates ( $2 \times 10^6$  cells/well) to 90% confluence, synchronized with serum-free DMEM for 24 hours, and then pretreated for 40 min with or without M10 or scrambled peptide. Next, cells were incubated with or without TGF $\beta$  (5ng/ml) for 20 min rapidly washed with ice-cold PBS and collected in 1x SDS sample buffer (100 $\mu\text{l}$ /well). Twenty  $\mu\text{l}$  of sample was separated on 4–20% SDS-polyacrylamide gels and immunoblotted with anti-phospho-Smad2 antibody. Total amount of Smad2 was evaluated by re-blotting with anti-Smad2 polyclonal antibody.

For immunoprecipitation assay, scleroderma skin and lung fibroblasts were grown to confluence on 100mm plates, kept in serum-free DMEM overnight, incubated with M10 for 24h, washed with ice cold PBS, and collected with 1ml of ice-cold solubilization buffer consisting of 10mM Tris-HCl, pH 7.4, 10mM EDTA, 150mM NaCl, 1% Nonidet P-40, 0.5% deoxycholate, 0.1% SDS. Samples were rotated for 3h and then cleared by microcentrifugation at 4°C. Next, anti-C12 antibody (1 $\mu\text{g}$ ) was added, and the samples were rotated for 90min at 4°C. Immune complexes were isolated on protein G-sepharose beads (Amersham Pharmacia Biotech, Piscataway, NJ), washed with buffer containing 10mM Tris-HCl, pH 7.4 and 10mM EDTA, resolved by gel electrophoresis, and immunoblotted with anti-Smad2 antibody.

### Protein Interaction Assay

DDK-tagged recombinant Smad2 and Smad4 were incubated with M10 (1µg each) in a total volume of 500 µl of Buffer A (20 mM Tris-HCl, pH 7.5, 0.6 mM EDTA, 70 mM NaCl, 0.01% Thesit) at 4 °C for 40 min with gentle rotation. C-12 antibody (1µg) was added, and incubation was continued for another 30 min followed by adding 50µl of protein G-sepharose slurry for an additional 20 minutes. The resin was washed three times with buffer A; the retained proteins were solubilized in Laemmli sample buffer and subjected to immunoblotting with anti-DDK monoclonal antibody.

### Bleomycin-induced model of lung fibrosis

Mice (n = 32), C57BL/6 male were used in this study. Mice were maintained in animal quarters specially designated for pathogen-free mice and were provided with food and water *ad libitum*. Lung injury was induced by intratracheal instillation of bleomycin (2U/kg in saline) under isoflurane anesthesia. Control mice received the same volume of saline. M10 (10 mg/kg) was administrated intraperitoneal every 48 hours. Control mice received 10 mg/kg of scrambled peptide. Animals were sacrificed in 3 weeks; lungs were harvested and processed for tissue staining and collagen measurements. All experimental procedures were performed according to guidelines of the Institutional Animal Care and Use Committee of the MUSC.

### Lung fixation and histological examinations

Sacrificed mice were subjected to midline thoracotomy. The trachea was cannulated, and the lungs were fixed by instillation of buffered formalin (2%) for 24 hours followed by perfusion with 70% ethanol for another 24 hours before routine processing and paraffin embedding as previously described.<sup>30</sup>

To evaluate the stages of lung fibrosis, multiple sections from each lung were stained with Hematoxylin and eosin (H & E staining) or with trichrome staining for collagen and other extracellular matrix proteins. Fibrosis quantification was performed by using 0 (normal) to 8 (total fibrosis) Ashcroft scale.<sup>31</sup> Morphological changes such as the thickness of alveolar septa, accumulation of vascular component and connective tissue, infiltration of inflammatory cells were analyzed. For histological evaluation each specimens were divided in 10 non-overlapping fields and scored independently. To avoid bias, all histological specimens were evaluated by three individuals in blinded fashion. The mean value from the individual score is presented as the fibrotic score.

### Collagen Assay

The total soluble collagen content was determined using Sircol Collagen Assay kit (Biocolor, Northern Ireland). The mouse lung was perfused with PBS to avoid blood saturation; left lobe was diced and digested overnight with 0.5M acetic acid and 0.2mg/ml pepsin. The soluble collagen was extracted by centrifugation (13000 g for 1hour at 4°C) and mixed with sircol dye reagent. After pelleting (13000 g for 10 min at room temperature), the samples were suspended in alkali reagent provided with the kit and read at 540nm by spectrophotometer.

## Statistical Analysis

Statistical analyses were performed with KaleidaGraph 4.0 (Synergy Software, Reading, PA). All data were analyzed using ANOVA with post-hoc testing. The results were considered significant if  $p < 0.05$ .

## Results

### M10 generation, intracellular localization, and effects on cell viability

M10 is a peptide comprising the last 10 amino acids (TRPASFWETS) of the HGF receptor, MET (Figure 1A). M10 is generated from MET's intracellular cytoplasmic tail upon cleavage by caspase-3. M10 has the chemical formula  $C_{53}H_{76}N_{14}O_{17}$ , a molecular weight of 1181.27 g/mol, and an isoelectric point at pH 6.97. Synthetic M10, obtained from GenScript (Piscataway, NJ) at pharmaceutical grade purity, is an off-white lyophilized powder that is well soluble in water. The hydropathy for each standard amino acid in the M10 peptide is shown in Figure 1B.

To investigate whether M10 affects cell viability, we employed two distinct cell viability assays performed in four primary cell lines (normal and scleroderma lung and skin fibroblasts) and two immortal cell lines (MRC5 and A549 cells). The ApoSENSOR™ cell viability assay is based on bioluminescent detection of the ATP levels in mammalian cells. Since cell death is an energy-dependent process that requires ATP, viable cells will be characterized by increased ATP levels. The assay utilizes luciferase to catalyze the formation of light from ATP and luciferin, and the relative light units (RLU) can be measured using a luminometer. We observed that the viability of control serum-starved cells was in a range of  $1.03 \times 10^6 - 3.04 \times 10^6$  RLU. M10 in concentrations of 1 µg/ml, 10 µg/ml, and 100 µg/ml did not affect cell viability in any of the six studied cell lines (Figure 1C) suggesting that M10 in the studied concentrations is not toxic for cells.

Similar results were obtained by Trypan blue cell counting. We found that cell counts of control and M10-treated viable cells were comparable ranging between  $2.12 \times 10^5 - 3.27 \times 10^5$  cells (Figure 1D) per well further suggesting lack of M10 toxicity in concentrations up to 100 µg/ml for fibroblasts and alveolar epithelial cells.

M10 contains at its N-terminus the uncharged amino acid proline (P) directly after a cationic amino acid arginine (R) which favors the transport of the peptide through membranes.<sup>33</sup> To follow the localization of M10 inside of cells we used an anti-Met C12 antibody, generated against the last 12 amino acids of MET, that recognizes M10 but does not recognize a scrambled peptide used as a control. Additionally, we used M10 directly conjugated with the red fluorescent marker 5,6-TAMRA at the N-terminus. We observed that following 24 hr of exposure M10 and 5,6-TAMRA-M10 are localized in the cytoplasm and nuclei of lung and skin fibroblasts (Figure 2).

### Effects of M10 on collagen in scleroderma and normal lung and skin fibroblasts

To determine whether M10 affects collagen expression in scleroderma fibroblasts, we incubated skin and lung fibroblasts isolated from six SSc patients with M10 and performed



Western blot analysis using anti-type I collagen antibody. As expected, SSc lung and skin fibroblasts demonstrated high levels of collagen expression at baseline. M10, added to the cells in a dose of 1 $\mu$ g/ml and 10 $\mu$ g/ml for 24 hours, effectively reduced collagen expression in a dose dependent manner in all six SSc lung and skin fibroblast cell lines (Figure 3 A and B). A scrambled peptide did not have any effect on collagen in any of the studied cell lines (Figure 3).

Next, we investigated whether M10 affects the levels of type I collagen in normal fibroblasts. Since normal fibroblasts contain less collagen as compared with scleroderma fibroblasts, we used TGF $\beta$  to stimulate collagen production. We observed that M10 at a concentration of 1 $\mu$ g/ml, but not a scrambled peptide, significantly reduced levels of TGF $\beta$ -induced collagen in fetal lung fibroblasts (MRC5 immortal cell line) and in primary normal lung and skin fibroblasts (( $p < 0.01$ ), Figure 4). Importantly, M10 had no effect on the basal levels of collagen in any of studied normal fibroblast cell lines.

### Investigation of M10 antifibrotic mechanism

Since M10 reduces TGF $\beta$ -stimulated collagen, we employed a computational modulation approach to explore possible interference of M10 with TGF $\beta$  signaling pathways. Using computational modeling available from PepSite: prediction of peptide-binding sites from protein surfaces,<sup>34</sup> we found a statistically significant ( $p < 0.02$ ) potential interaction of M10 with the Mad Homology (MH)2 domain of Smad2 (Figure 5A). To confirm the predicted M10/Smad2 interaction, we performed a set of peptide-protein interaction experiments using synthetic M10 and recombinant human Smad2 tagged with DDK. As negative controls in these experiments, we used M10 incubated with DDK-tagged Smad4 and scrambled peptide incubated with DDK-tagged Smad2. As a positive control for anti-DDK antibody, we loaded to the gel 5 $\mu$ l-aliquots of a buffer containing DDK-tagged recombinant Smad2 or Smad4 proteins. We observed that M10 interacts with Smad2, but not with Smad4, and that scrambled peptide does not interact with Smad2 or with Smad4 (Figure 5B).

Next, we performed co-immunoprecipitation experiments to test whether M10 and Smad2 actually interact in lung and skin fibroblasts. For these experiments, we used scleroderma lung and skin primary fibroblasts characterized by high expression of endogenous Smad2. We confirmed an interaction of Smad2 with M10 in both lung and skin fibroblasts that were treated with M10, but not in cells treated with a scrambled peptide (Figure 5C).

To further investigate the interaction of M10 with Smad2, we studied co-localization of M10 and Smad2 in primary lung fibroblasts in the presence and absence of TGF $\beta$ . We found that M10 and Smad2 co-localize with or without TGF $\beta$  treatment. Interestingly, without TGF $\beta$  treatment M10 and Smad2 are distributed in the cytoplasm and nuclei of these cells. However, after TGF $\beta$  treatment M10 and Smad2 accumulate and co-localize mostly in the nuclei of these cells (Figure 6A).

TGF $\beta$  leads to the phosphorylation of Smad2. To determine whether M10 interferes with TGF $\beta$ -induced Smad2 phosphorylation, we studied TGF $\beta$ -induced Smad2 phosphorylation in the presence and absence of M10 in lung and skin fibroblasts. We observed that within 20 min of TGF $\beta$  stimulation, Smad2 phosphorylation was significantly increased as compared

to unstimulated cells. M10, at a concentration of 1 µg/ml, decreased TGFβ-induced Smad2 phosphorylation but did not affect the basal level of phospho-Smad2 or total Smad2 (Figure 6B).

### **Histologic evaluation of anti-inflammatory and antifibrotic effects of M10 in a bleomycin murine model of pulmonary fibrosis**

In control mice that received saline and scrambled peptide or saline and M10, lung histology was characterized by alveolar structures composed of normal septa, vascular components, and connective tissue. Lung tissue isolated from bleomycin-treated mice demonstrated extensive peribronchial and interstitial infiltration of inflammatory cells, thickening of the alveolar walls, and multiple focal fibrotic lesions with excessive amounts of ECM protein. In contrast, significantly fewer cellular infiltrates, decreased thickness of alveolar septa and reduced accumulation of ECM proteins were noted in mice treated with M10 (Figure 7A).

The overall level of fibrotic changes was quantitatively assessed based on the Ashcroft scoring system.<sup>31</sup> The Ashcroft score in saline-administrated M10-treated control mice was similar to saline-administrated control mice treated with scrambled peptide ( $0.65\pm 0.37$  and  $0.69\pm 0.35$  respectively). The Ashcroft fibrosis score in mice treated with bleomycin and scrambled peptide reached  $5.63\pm 1.72$  or about 8.2-fold higher as compared with controls. The Ashcroft fibrosis score in bleomycin challenged mice treated with M10 was reduced to  $1.67\pm 1.01$ , reflecting a pronounced antifibrotic effect of M10 ( $p<0.05$ ) (Figure 7B).

### **Effect of M10 on collagen accumulation in bleomycin-induced pulmonary fibrosis**

To quantify collagen accumulation within the lungs we employed Sircol collagen assay. This assay is a direct quantitative method for the analysis of collagens based on the reagent Sirius Red that reacts specifically with the side chain groups of the basic amino acids present in collagen. We observed that total soluble collagen content in M10-treated control mice was similar to saline-administrated control mice ( $9.4\pm 2.1$  µg/mg of lung and  $9.6\pm 3.9$  µg/mg of lung, respectively). Collagen content in bleomycin and scrambled peptide treated mice was increased more than 4-fold compared with control. Bleomycin-treated mice receiving M10 were characterized by over 50% reduction of the total soluble collagen when compared with bleomycin-challenged mice treated with a scrambled peptide (Figure 7C).

## **Discussion**

Small peptides are widely involved in multiple cellular events and play very important roles in various cell functions. Interest in peptides as potential drug candidates remains high. With advances in such fields as chemical synthesis and peptide formulation, peptide drugs - especially short synthetic and long-acting peptides - are quickly increasing in the global market.<sup>32</sup> The advantages of small peptides as drugs include their high biological activity, high specificity, and low toxicity.<sup>34</sup> Highly effective treatment for scleroderma-associated pulmonary fibrosis and other important fibrosing diseases is lacking, which makes identification of a peptide with antifibrotic properties a potentially very exciting and important discovery for this and other fibrosing diseases.



We recently discovered a small ten amino acid peptide, “M10”, which is derived from the C-terminal part of the MET receptor tyrosine kinase via naturally occurring caspase-3 mediated cleavage.<sup>7</sup> We reported that MET can generate M10 without HGF stimulation and that the MET D1398G mutant is incapable of generating M10, as aspartic acid at position 1398 is necessary for caspase-3 cleavage.<sup>7</sup> The present study was designed to investigate the antifibrotic effects of M10 in lung and skin fibroblasts isolated from SSc patients.

Since M10 is an intracellular fragment of MET, we hypothesized that its primary effects would be exerted inside of cells. Translocation of peptides through the cell membrane in general can occur via endocytosis or through direct diffusion in an energy independent manner mediated by membrane potential.<sup>35</sup> M10 is a 10-mer peptide containing at its N-terminus the uncharged amino acid proline directly following a cationic amino acid arginine, which favors the transport of the peptide through membranes.<sup>32</sup> This composition of amino acids within M10 suggests that the peptide can easily penetrate the lipid bilayers not only of the cell membrane, but also of the nuclear membrane. In agreement with this, using immunofluorescence we observed M10 in cytoplasm and nuclei of fibroblasts. Since the C12 antibody employed in these experiments can recognize not only M10 but also uncleaved MET, we additionally used direct coupling of M10 to a fluorophore (5,6-TAMRA) to evaluate the distribution of M10 in fibroblasts. Patterns of M10 localization within cells were identical when detected by the fluorescent signals generated by C12 antibody or by those produced by the fluorophore 5,6-TAMRA, which suggests that M10's intracellular location can be either intracytoplasmic or intranuclear.

Excessive expression of collagen is a hallmark of scleroderma and other fibrotic diseases, and TGF $\beta$  is the main fibrogenic cytokine stimulating production of collagen in fibroblasts.<sup>36</sup> Therefore, we tested synthetic M10 for its effect on collagen expression in lung and skin fibroblasts isolated from SSc patients and in TGF $\beta$ -stimulated normal lung and skin fibroblasts. We found that M10 diminished collagen in SSc lung and skin fibroblasts *in vitro*. Importantly, M10 reduced TGF $\beta$ -induced collagen type I in normal fibroblast and had no effects on basal levels of collagen, which suggests that M10 interferes with TGF $\beta$ -dependent fibrogenic pathways in fibroblasts.

TGF $\beta$  signaling in fibroblasts plays a major pathogenic role in SSc and other fibrosing diseases. Most of TGF $\beta$ -induced signal transduction is mediated intracellularly by Smad proteins, including receptor-regulated (R)-Smads (Smad2 and Smad3), common (Co)-Smad (Smad4), and inhibitory (I)-Smads (Smad6 and Smad7). Smads are intracellular proteins that act as transcription factors to regulate gene expression.<sup>37</sup> They consist of a conserved N-terminal MH1 domain and a C-terminal MH2 domain connected by a linker region.<sup>37</sup> The MH2 domain can interact with a diverse group of proteins including membrane anchoring proteins and transcription factors.<sup>38</sup>

Peptide-mediated interactions, in which a short linear motif binds to a globular domain, play major roles in many biological processes, such as protein localization, endocytosis, post-translational modifications, and signal transduction.<sup>39</sup> Using computational modulation, we found that the MH2 domain of Smad2 protein could interact with our M10 peptide. Herein, we confirm this by protein interaction and co-immunoprecipitation experiments.

Additionally, using immunofluorescent studies we show that M10 co-localizes with Smad2 in cytoplasm and in nuclei in the presence of TGF $\beta$ , suggesting that this interaction is quite persistent and might be involved in the regulation of Smad2 functions.

In addition to the peptide interaction with Smad2, M10 reduces TGF $\beta$ -induced phosphorylation of Smad2 in skin and lung fibroblasts. As Smad2 phosphorylation is essential for TGF $\beta$ -regulated synthesis of collagen,<sup>40</sup> inhibition of Smad2 phosphorylation might be one of the mechanisms by which M10 exerts its antifibrotic effects.

Pulmonary fibrosis is a severe complication and a major cause of mortality in patients with scleroderma.<sup>41, 42</sup> To explore antifibrotic effects of M10 *in vivo*, we employed a model of pulmonary fibrosis using a single intratracheal administration of bleomycin in mice. We observed that treatment with M10 by intraperitoneal injection markedly improved bleomycin-induced fibrosis, suggesting that M10 peptide may have potential for use in the treatment of scleroderma-associated ILD and other forms of pulmonary fibrosis, *e.g.*, idiopathic pulmonary fibrosis (IPF). One limitation of our study is that we started M10 treatment on the same day as bleomycin was administered. It is established that drugs administered during the early injury phase predominantly act as anti-inflammatory agents and should be considered as “preventive treatment”, whereas “true” antifibrotic agents might be effective irrespective of timing, particularly if administered during the “fibrotic” phase of the model.<sup>43</sup> We plan to perform a study in which both early and late treatments with M10 will be investigated.

There is a great need for more effective therapy for SSc-ILD as well as other fibrosing diseases. In fact, fibrotic diseases account for up to 45% of deaths in the developed world, yet there are no approved antifibrotic therapies.<sup>44</sup> Peptide drugs have been successfully used for many diseases for over forty years.<sup>45</sup> Peptides offer certain advantages as drugs including high biological activity, high specificity, and low toxicity. As demonstrated herein, the *in vitro* and *in vivo* antifibrotic effects of M10 are very promising and further development may lead to more effective therapy for patients who suffer from SSc and other fibrosing diseases.

## Acknowledgments

This study is funded by the Multidisciplinary Clinical Research Center grant from the National Institute of Arthritis and Musculoskeletal and Skin Diseases (P60 AR062755 to GSB and RMS) and by the South Carolina Clinical & Translational Research (SCTR) Institute, with an academic home at the Medical University of South Carolina, through NIH - NCATS Grant Number UL1 TR000062. Imaging core is supported by South Carolina COBRE for Developmentally Based Cardiovascular Diseases (NIH-NIGMS P30 GM103342).

All authors have read the journal’s authorship statement and the journal’s policy on disclosure of potential conflicts of interest. None of the authors has any financial or personal relationship with organizations that could potentially be perceived as influencing the described research.

A provisional patent application was filed July 28, 2015, covering the M10 peptide as a therapeutic for fibrosis.

## Abbreviations

**HGF**                      Hepatocyte growth factor

|                   |  |
|-------------------|--|
| <b>c-MET, MET</b> | mesenchymal-epithelial transition factor |
| <b>SSc</b>        | scleroderma systemic sclerosis           |
| <b>ILD</b>        | interstitial lung disease                |
| <b>IPF</b>        | idiopathic pulmonary fibrosis            |

## References

1. Castellino FV, Varga J. Emerging cellular and molecular targets in fibrosis: implications for scleroderma pathogenesis and targeted therapy. *Curr Opin Rheumatol.* 2014; 26(6):607–14. [PubMed: 25191991]
2. McMahan ZH, Wigley FM. Novel investigational agents for the treatment of scleroderma. *Expert Opin Investig Drugs.* 2014; 23(2):183–98.
3. Inoue T, Okada H, Kobayashi T, et al. Hepatocyte growth factor counteracts transforming growth factor-beta1, through attenuation of connective tissue growth factor induction, and prevents renal fibrogenesis in 5/6 nephrectomized mice. *FASEB J.* 2003; 17:268–70. [PubMed: 12475893]
4. Mizuno S, Matsumoto K, Li MY, Nakamura T. HGF reduces advancing lung fibrosis in mice: a potential role for MMP-dependent myofibroblast apoptosis. *FASEB J.* 2005; 19(6):580–2. [PubMed: 15665032]
5. Gazdhar A, Temuri A, Knudsen L, et al. Targeted gene transfer of hepatocyte growth factor to alveolar type II epithelial cells reduces lung fibrosis in rats. *Hum Gene Ther.* 2013; 24(1):105–16. [PubMed: 23134111]
6. Bogatkevich GS, Ludwicka-Bradley A, Highland KB, et al. Impairment of the antifibrotic effect of hepatocyte growth factor in lung fibroblasts from African Americans: possible role in systemic sclerosis. *Arthritis Rheum.* 2007; 56:2432–42. [PubMed: 17599773]
7. Atanelishvili I, Akter T, Silver RM, Bogatkevich GS. D1398G variant of hepatocyte growth factor receptor – a potential biomarker of severe interstitial lung disease in African American scleroderma patients. *Arthritis Rheum.* 2013; 65(10 Suppl):2907. [PubMed: 23918739]
8. Giordano S1, Di Renzo MF, Narsimhan RP, Cooper CS, Rosa C, Comoglio PM. Biosynthesis of the protein encoded by the c-met proto-oncogene. *Oncogene.* 1989; 4(11):1383–8. [PubMed: 2554238]
9. Skead G, Govender D. Gene of the month: MET. *J Clin Pathol.* 2015; 68(6):405–409. [PubMed: 25987653]
10. Vigna E, Naldini L, Tamagnone L, et al. Hepatocyte growth factor and its receptor, the tyrosine kinase encoded by the c-MET proto-oncogene. *Cell Mol Biol.* 1994; 40:597–604. [PubMed: 7981617]
11. Orian-Rousseau V, Chen L, Sleeman JP, Herrlich P, Ponta H. CD44 is required for two consecutive steps in HGF/c-Met signaling. *Genes Dev.* 2002; 16:3074–3086. [PubMed: 12464636]
12. Ghatak S, Bogatkevich GS, Atnelishvili I, et al. Overexpression of c-Met and CD44v6 receptors contributes to autocrine TGF-β1 signaling in interstitial lung disease. *J Biol Chem.* 2014; 289(11):7856–72. [PubMed: 24324260]
13. Trusolino L, Bertotti A, Comoglio PM. A signaling adapter function for alpha6beta4 integrin in the control of HGF-dependent invasive growth. *Cell.* 2001; 107:643–654. [PubMed: 11733063]
14. Accordi B, Pillozzi S, Dell’Orto MC, et al. Hepatocyte growth factor receptor c-MET is associated with FAS and when activated enhances drug-induced apoptosis in pediatric B acute lymphoblastic leukemia with TEL-AML1 translocation. *J Biol Chem.* 2007; 282(40):29384–93. [PubMed: 17673463]
15. Giordano S, Corso S, Conrotto P, et al. The semaphorin 4D receptor controls invasive growth by coupling with Met. *Nat Cell Biol.* 2002; 4:720–724. [PubMed: 12198496]
16. Kawaguchi Y, Harigai M, Hara M, et al. Expression of hepatocyte growth factor and its receptor (c-met) in skin fibroblasts from patients with systemic sclerosis. *J Rheumatol.* 2002; 29:1877–83. [PubMed: 12233882]

17. Tokunou M, Niki T, Eguchi K, et al. c-MET expression in myofibroblasts: role in autocrine activation and prognostic significance in lung adenocarcinoma. *Am J Pathol.* 2001; 158:1451–63. [PubMed: 11290563]
18. Foveau B, Leroy C, Ancot F, Deheuninck J, Ji Z, Fafeur V, Tulasne D. Amplification of apoptosis through sequential caspase cleavage of the MET tyrosine kinase receptor. *Cell Death Differ.* 2007; 14(4):752–64. [PubMed: 17186028]
19. Kim WH, Matsumoto K, Bessho K, Nakamura T. Growth inhibition and apoptosis in liver myofibroblasts promoted by hepatocyte growth factor leads to resolution from liver cirrhosis. *Am J Pathol.* 2005; 166(4):1017–28. [PubMed: 15793283]
20. Mizuno S, Matsumoto K, Li MY, Nakamura T. HGF reduces advancing lung fibrosis in mice: a potential role for MMP-dependent myofibroblast apoptosis. *FASEB J.* 2005; 19(6):580–2. [PubMed: 15665032]
21. Slee EA, Adrain C, Martin SJ. Executioner caspase-3, -6, and -7 perform distinct, non-redundant roles during the demolition phase of apoptosis. *J Biol Chem.* 2001; 276(10):7320–6. [PubMed: 11058599]
22. Woo M, Hakem R, Furlonger C, et al. Caspase-3 regulates cell cycle in B cells: a consequence of substrate specificity. *Nat Immunol.* 2003; 4(10):1016–22. [PubMed: 12970760]
23. De Botton S, Sabri S, Daugas E, et al. Platelet formation is the consequence of caspase activation within megakaryocytes. *Blood.* 2002; 100(4):1310–7. [PubMed: 12149212]
24. Okazaki S, Ogawa F, Iwata Y, et al. Autoantibody against caspase-3, an executioner of apoptosis, in patients with systemic sclerosis. *Rheumatol Int.* 2010; 30(7):871–8. [PubMed: 19639321]
25. Lefebvre J, Muharram G, Leroy C, et al. Caspase-generated fragment of the Met receptor favors apoptosis via the intrinsic pathway independently of its tyrosine kinase activity. *Cell Death Dis.* 2013; 4:e871. [PubMed: 24136235]
26. Ma J, Zou C, Guo L, et al. Novel Death Defying Domain in Met entraps the active site of caspase-3 and blocks apoptosis in hepatocytes. *Hepatology.* 2014; 59(5):2010–21. [PubMed: 24122846]
27. Van den Hoogen F, Khanna D, Fransen J, et al. 2013 classification criteria for systemic sclerosis: an American College of Rheumatology/European League against Rheumatism collaborative initiative. *Arthritis Rheum.* 2013; 65:2737–47. [PubMed: 24122180]
28. Bogatkevich GS, Tourkina E, Silver RM, Ludwicka-Bradley A. Thrombin differentiates normal lung fibroblast to a myofibroblast phenotype via proteolytically activated receptor-1 and protein kinase C-dependent pathway. *J Biol Chem.* 2001; 276:45184–92. [PubMed: 11579091]
29. Bogatkevich GS, Ludwicka-Bradley A, Highland KB, et al. Down-regulation of collagen and connective tissue growth factor expression with hepatocyte growth factor in lung fibroblasts from white scleroderma patients via two signaling pathways. *Arthritis Rheum.* 2007; 56:3468–77. [PubMed: 17907155]
30. Bogatkevich GS, Ludwicka-Bradley A, Nietert PJ, Akter T, van Ryn J, Silver RM. Anti-inflammatory and antifibrotic effects of the oral direct thrombin inhibitor dabigatran etexilate in a murine model of interstitial lung disease. *Arthritis Rheum.* 2011; 63(5):1416–25. [PubMed: 21312187]
31. Ashcroft T, Simpson JM, Timbrell V. Simple method of estimating severity of pulmonary fibrosis on a numerical scale. *J Clin Pathol.* 1988; 41:467–470. [PubMed: 3366935]
32. Fonseca SB, Pereira MP, Kelley SO. Recent advances in the use of cell-penetrating peptides for medical and biological applications. *Adv Drug Deliv Rev.* 2009; 61:953–64. [PubMed: 19538995]
33. Trabuco LG, Lise S, Petsalaki E, Russell RB. PepSite: prediction of peptide-binding sites from protein surfaces. *Nucleic Acids Res.* 2012; 40:W423–7. [PubMed: 22600738]
34. Craik DJ, Fairlie DP, Liras S, Price D. The future of peptide-based drugs. *Chem Biol Drug Des.* 2013; 81(1):136–47. [PubMed: 23253135]
35. Choi YS, David AE. Cell penetrating peptides and the mechanisms for intracellular entry. *Curr Pharm Biotechnol.* 2014; 15(3):192–9. [PubMed: 24938895]
36. Varga J, Whitfield ML. Transforming growth factor-beta in systemic sclerosis (scleroderma). *Front Biosci (Schol Ed).* 2009; 1:226–35. [PubMed: 19482698]
37. Hill CS. The Smads. *Int J Biochem Cell Biol.* 1999; 31(11):1249–54. [PubMed: 10605817]

38. Chacko BM, Qin BY, Tiwari A, et al. Structural basis of heteromeric smad protein assembly in TGF-beta signaling. *Mol Cell*. 2004; 15(5):813–23. [PubMed: 15350224]
39. London N, Movshovitz-Attias D, Schueler-Furman O. The structural basis of peptide-protein binding strategies. *Structure*. 2010; 18(2):188–99. [PubMed: 20159464]
40. Ishida W, Mori Y, Lakos G, et al. Intracellular TGF-beta receptor blockade abrogates Smad-dependent fibroblast activation in vitro and in vivo. *J Invest Dermatol*. 2006; 126(8):1733–44. [PubMed: 16741519]
41. Bogatkevich GS. Lung involvement in scleroderma. *Rheumatol Curr Res*. 2012; S1:e001.
42. Fan MH, Feghali-Bostwick CA, Silver RM. Update on scleroderma-associated interstitial lung disease. *Curr Opin Rheumatol*. 2014; 26(6):630–6. [PubMed: 25191993]
43. Moeller A, Ask K, Warburton D, Gaudie J, Kolb M. The bleomycin animal model: a useful tool to investigate treatment options for idiopathic pulmonary fibrosis? *Int J Biochem Cell Biol*. 2008; 40(3):362–82. [PubMed: 17936056]
44. Wynn TA. Cellular and molecular mechanisms of fibrosis. *J Pathol*. 2008; 214(2):199–210. [PubMed: 18161745]
45. Vlieghe P, Lisowski V, Martinez J, Khrestchatisky M. Synthetic therapeutic peptides: science and market. *Drug Discov Today*. 2010; 15:40–56. [PubMed: 19879957]

### Background

The molecular mechanisms underlying the pathogenesis of fibrosis are not well understood, and treatment is often toxic and inefficacious. Earlier studies have identified hepatocyte growth factor (HGF) as an antifibrotic agent that protects various tissues including lung from injury and fibrosis.



### **Translational Significance**

Recently we identified a C-terminal fragment of HGF receptor, M10, as a peptide with strong antifibrotic properties. This is the first manuscript to describe antifibrotic effects of M10 in vitro and in vivo that can be translated into a safe and effective treatment of pulmonary fibrosis and other fibrosing diseases.

Author Manuscript

Author Manuscript

Author Manuscript

Author Manuscript

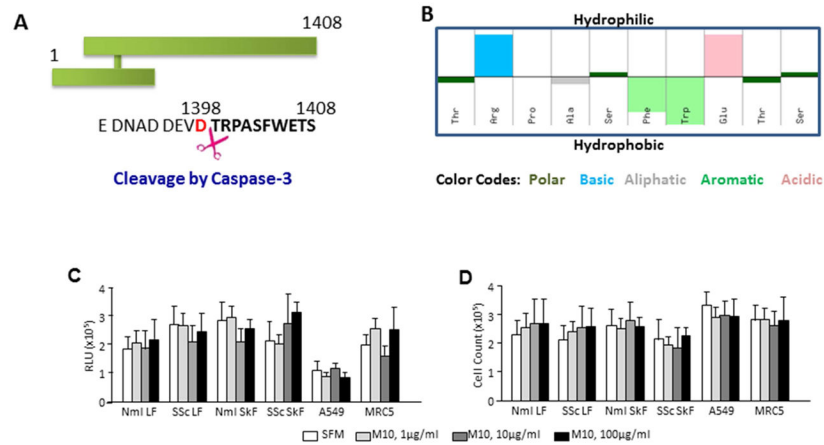


**Figure 1. Basic properties of M10 peptide**

**A**, Position of M10 on the MET receptor tyrosine kinase. Cleavage site of caspase 3 is indicated by scissors. **B**, Hydropathy plot of M10 is prepared by the Hopp–Woods hydrophilicity scale. Hydrophilic residues are presented as upward bars and hydrophobic residues are presented as downward bars. **C and D**, M10 does not affect cell viability measured by the ATP-dependent assay (**C**) and by trypan blue cell counting (**D**).

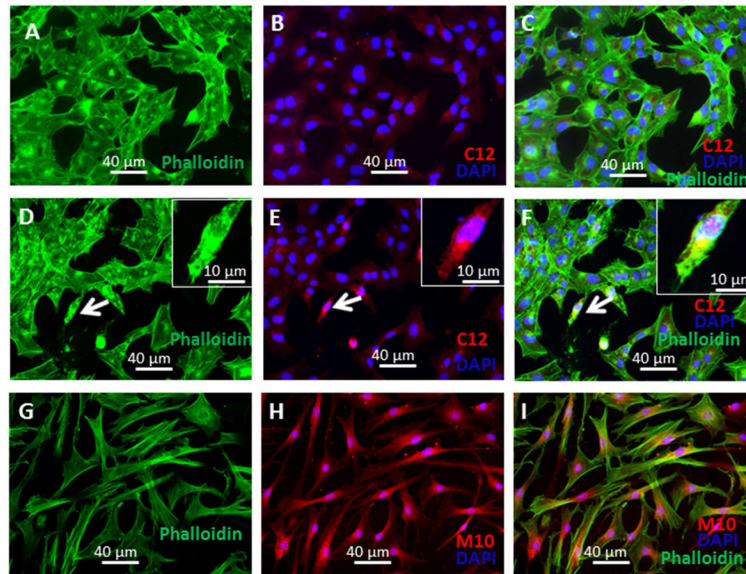


**Figure 2. Intracellular localization of M10**

**A–F**, Lung fibroblasts were seeded on 4-chamber slides, serum-starved for 24 h followed by incubation for 24 h with M10 or scrambled peptide (10 μg/ml). Cells were fixed with 4% formaldehyde and stained with anti-Met (C12) antibody (**A–F**), or incubated with TAMRA-conjugated M10 (**G–I**). After labeling slides were mounted by Gold anti-fade reagent with Phalloidin and DAPI and visualized using a Leica DMI4000B fluorescence microscope equipped with Hamamatsu Camera Controller ORCA-ER.

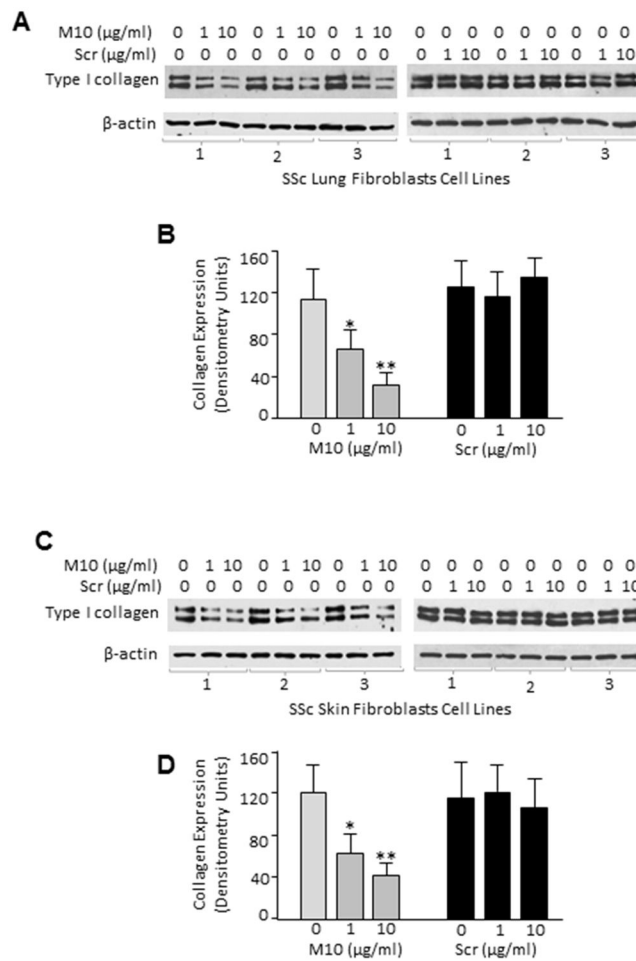


**Figure 3. Concentration-dependent effect of M10 on the expression of collagen type I in scleroderma lung and skin fibroblasts**

**A and C**, SSc lung and skin fibroblasts were serum-starved for 24 h followed by incubation for 48 h with indicated concentrations of M10 or scrambled peptide (Scr). Cells were collected with lysis buffer and analyzed by Western blot with anti-collagen type I and anti- $\beta$ -actin antibody as a loading control. **B and D**, Densitometric analysis of immunoblots. Values are the mean and SD from three independent experiments. \* =  $P < 0.05$  and \*\* =  $P < 0.01$  versus unstimulated cells.



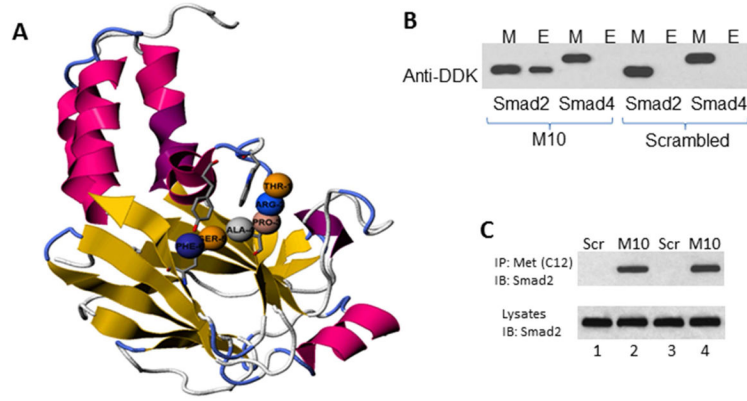


**Figure 5. M10 and Smad2 interaction**

**A**, M10 in complex with Smad2. The interactive visualization of statistically significant ( $p < 0.02$ ) binding of M10 (amino acids pro-3, ala-4, trp-7, glu-8, thr-9, and ser-10) with MH2 domain of Smad2. **B**, M10 interacts with Smad2 but not Smad4. DDK-tagged recombinant Smad2 and Smad4 were incubated with M10 as detailed in the Materials and Methods. Interacting complexes were captured with Protein G sepharose and subjected to immunoblotting with anti-DDK antibody. Peptide-protein interacting mixture (M) was used as a positive control. E stands for Eluted Interacting Complexes. **C**, Co-immunoprecipitation of M10 and Smad2 in scleroderma lung (lanes 1 and 2) and skin (lanes 3 and 4) fibroblasts. Cells were cultured in 100 mm plates to confluence, serum-starved overnight, incubated with M10 or scrambled peptide (Scr) for 24 h, collected, and subjected to immunoprecipitation as outlined in the experimental procedures.



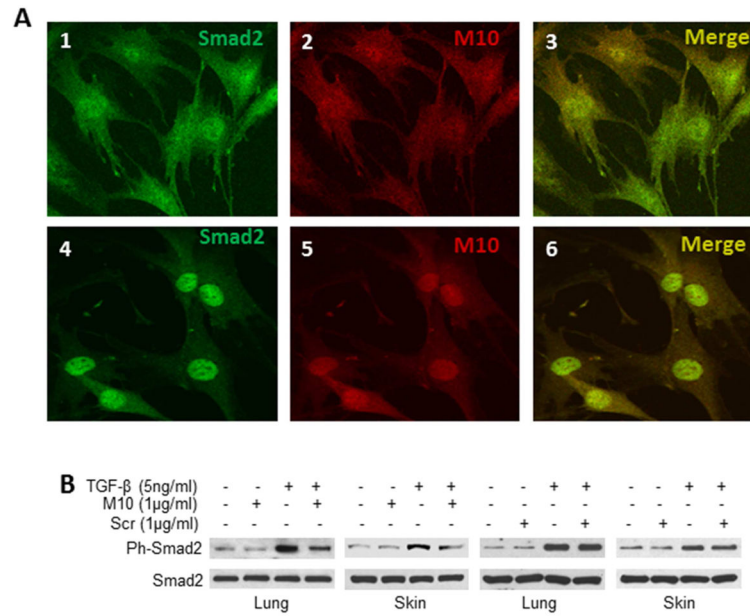


**Figure 6. M10 co-localizes with Smad2 and inhibits TGF $\beta$ -induced Smad2 phosphorylation**  
**A**, Co-localization of Smad2 and M10 in lung fibroblasts cultured in serum free medium without TGF $\beta$  (panels 1, 2, and 3) and with TGF $\beta$  (panels 4, 5, and 6). **B**, M10 reduces TGF $\beta$ -induced Smad2 phosphorylation in normal lung and skin fibroblasts. Cells were cultured on 6-well plates to 90% confluence, serum-starved overnight, incubated with or without M10 or scrambled peptide (Scr) and TGF $\beta$ , and subjected to immunoblotting as detailed in the Methods section.

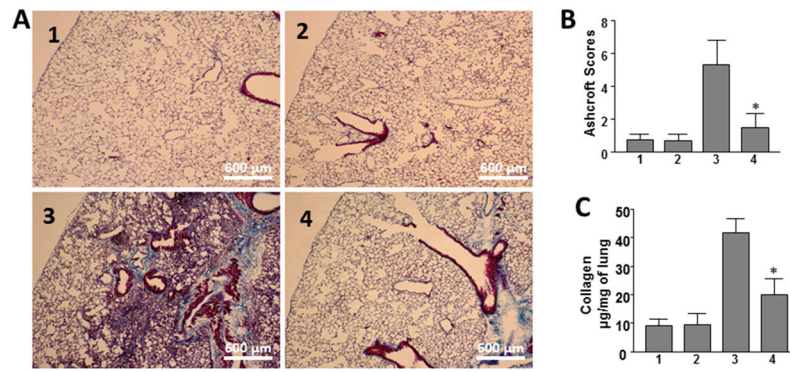


**Figure 7. Effect of M10 on bleomycin-induced pulmonary fibrosis**

**A.** Representative histological findings of lung inflammation and fibrosis. 1 – control 1 (saline + scrambled peptide), 2 – control 2 (saline + M10), 3 bleomycin + scrambled peptide, 4 – bleomycin + M10. **B.** Quantitative evaluation of fibrotic changes (Ashcroft scores),  $n = 32$  (eight mice per group). **C.** Lung collagen content determined by Sircol assay,  $n = 24$  (six mice per group). Values in **B** and **C** are the mean  $\pm$  SD. \*statistically significant differences ( $P < 0.05$ ) between bleomycin challenged mice treated with M10 and scrambled peptide.